



International Operational Modal Analysis Conference

20 - 23 May 2025 | Rennes, France

Structural damage detection on a full-scale masonry cross-vault subjected to quasi-static cyclic loading tests

Alejandro Bendezu¹, Daniele Pellegrini² and César Chácará³

¹ Engineering Department, Pontificia Universidad Católica del Perú, alejandro.bendezu@pucp.edu.pe

² National Research Council of Italy, Institute of Information Science and Technologies "A. Faedo", daniele.pellegrini@isti.cnr.it

³ Engineering Department, Pontificia Universidad Católica del Perú, c.chacara@pucp.edu.pe

ABSTRACT

This paper presents the results of an experimental campaign for structural damage detection on a full-scale alternative-masonry cross-vault subjected to quasi-static cyclic tests. The masonry constituent material was composed of stabilised compressed earth blocks and soil-cement mortar. The cross-vault specimen presented a square plan with a span of approximately 3.20 m. Its boundary conditions consisted of two fixed corners that restrained displacements and rotations in all directions, and two corners that were placed over four-wheeled steel masses that enabled horizontal displacements. The masonry cross-vault was subjected to incremental horizontal cyclic load following a displacement-controlled approach to capture its in-plane shear failure. A total of 14 cyclic load sequences were applied to the specimen, reaching a maximum displacement of about 40 mm. The damage detection was evaluated in terms of frequency decrease and modal shape variations, estimated by operational modal analyses (OMA) technique carried out every two cyclic loads sequences considering ambient vibrations as excitation source. The Enhanced Frequency Domain Decomposition (EFDD) method implemented in the ARTeMIS Modal software estimated the specimen's frequencies. The results show an important decay in natural frequencies and variations of the first three mode shapes, especially when the vault experienced severe damage.

Keywords: Compressed earth blocks masonry, In-plane shear failure mechanism, Damage scenarios, Dynamic properties, Operational modal analysis.

1. INTRODUCTION

Masonry cross-vaults are structural elements usually found in the roofing systems of historical and architectural landmarks such as churches and monasteries. The complex geometrical characteristics and weak mechanical properties of this structural typology make them significantly vulnerable to

external loading, such as earthquakes. In this regard, a comprehensive understanding of these elements' structural and seismic behaviour is essential. As reported in the Italian manual for damage identification in churches [1], one of the typical failure mechanisms of cross-vaults is in-plane shear deformation caused by the relative displacement of masonry walls and pillars. In the last years, the seismic response of masonry cross-vaults has been addressed by experimental [2], [3] and numerical [4], [5] studies. For instance, Bianchini et al. [2] conducted shaking table tests on unreinforced and reinforced specimens to investigate shear-induced damage patterns and collapse mechanisms. However, limited studies that focused on assessing the influence of structural damage on the dynamic properties of these elements can be found in literature. In this study, the damage detection on a full-scale masonry cross-vault was assessed considering the application of incremental quasi-static cyclic loading. The masonry cross-vault was made of an alternative system composed of compressed earth block (CEB) stabilised with cement and lime together with cement-based mortar joints. The boundary conditions of the specimen consisted of fixed and movable edges that enabled in-plane shear failure mechanisms, taking as reference the work carried out by Bianchini et al. [2]. The cyclic behaviour of the cross-vault was evaluated in terms of hysteretic curves and crack patterns, whereas damage detection was investigated by estimating changes in dynamic properties. For this purpose, a set of Operational Modal Analyses (OMA) was applied to the CEB masonry cross-vault under a no-damage condition (reference scenario RS) and at seven incremental damage scenarios DSs. The ambient vibrations were processed using a frequency-domain technique, the Enhanced Frequency Domain Decomposition (EFDD) method [6], implemented in the software ARTEMIS Modal. The first three vibration modes were studied through natural frequencies and mode shapes. The damage detection of the vault was evaluated by comparing the natural frequencies and Modal Assurance Criterion (MAC) for the mode shapes between consecutive DSs. A strong correlation was observed between damage progression and the reduction in frequencies and MAC values for all three vibration modes.

2. EXPERIMENTAL SETUP

2.1. Masonry cross-vault

The cross-vault considered for this research was constituted by an alternative masonry system composed of CEB proposed by Huamani et al. [7] and cement-based mortar joints. As reported in Huamani et al. [7], the CEB was stabilised with Portland Type I cement and lime in a 9:1 ratio. The resulting block presented average dimensions of 280 mm in length, 140 mm in width and 75 mm in height. On the other hand, the material used for the 10 mm-thick head and bed joints was made of a soil-cement mix considering a ratio equal to 4:1. The geometry of the cross-vault was symmetrical and described by four arches with an inner diameter of 3.00 m and a sweep angle of 120°. Based on these parameters, the resulting overall dimensions of the cross-vault were 3.20 m in length and width and 0.90 m in height. CEB masonry infills, with an approximate height of 500 mm, were built on each corner of the specimen aiming at improving their stability. Based on the boundary conditions implemented in the work of Bianchini et al. [2], two corners of the cross-vault were supported by two CEB masonry piers, whereas the remaining two were placed on top of two four-wheeled steel masses (see Figure 1).

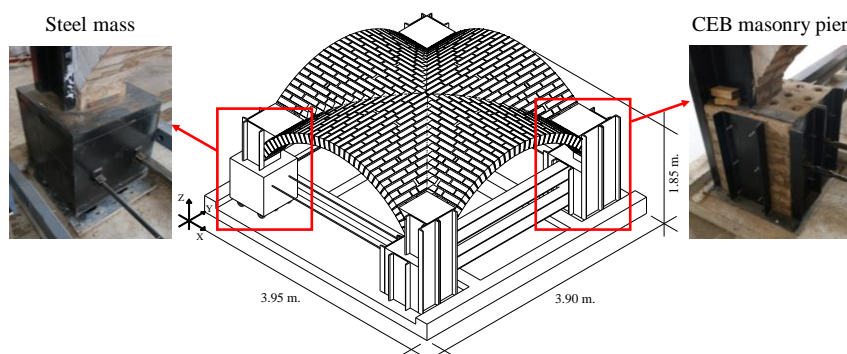


Figure 1. Cross-vault mock-up: different types of supports and overall dimensions are displayed.

The masonry piers were considered fixed supports blocked by steel profiles used to restrain displacements and rotations in all directions. To this aim, vertical U-shaped steel profiles were incorporated into the infills and piers, and two horizontal W-shaped profiles were connected to both fixed masonry piers. The steel masses were considered movable supports since the wheels enabled the relative horizontal displacement of the specimen. Finally, 1-inch diameter steel bars were used to connect the mobile and fixed supports. These elements presented a pinned connection at their ends to prevent torsional effects.

2.2. Loading mechanism

A servo-controlled actuator was used to apply the cyclic loading to one of the mobile supports (see Figure 2a). The application of the cyclic load required a proper connection between the actuator and the movable support. For this purpose, an easy-to-assemble device consisting of rectangular steel profiles was designed: one welded to the back of the movable supports and the other mounted on the actuator. Steel bars were inserted through aligned holes and secured with bolts to ensure contact between the actuator and the movable support and enable efficient load transmission (see Figure 2b).

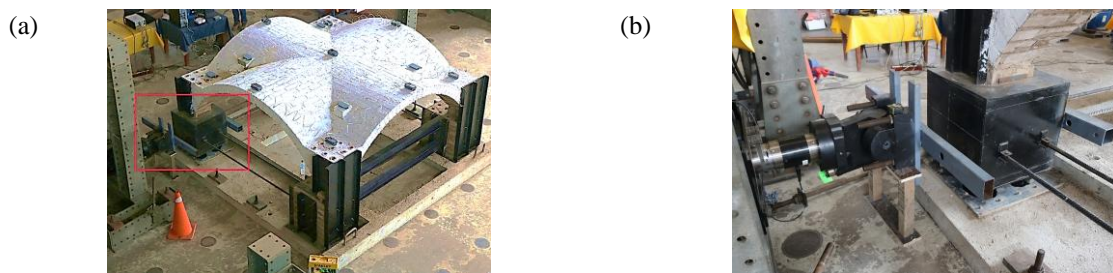


Figure 2. Cyclic loading mechanism. (a) displacement application setup, and (b) actuator-support connection.

2.3. Instrumentation

The transducers used to measure the mock-up's vibrations consisted of eight triaxial DEWESoft® IOLITEiw-3xMEMS-ACC-INC accelerometers characterised by a noise density of $25 \mu\text{g}/\sqrt{\text{Hz}}$, and a dynamic range of $\pm 2\text{g}$. The experiments considered two different instrumentation setups in which the sensors were strategically placed on the extrados of the CEB masonry cross-vault. Three sensors were kept fixed for both setups, and were located on top of the masonry infills of each movable support and on the centre of the cross-vault. The remaining five sensors were placed on top of the infills of the fixed supports and on the shell of the cross-vault. It is worth noting that the measurement of the ambient vibrations in the Z-direction was neglected in the case of the sensors located on top of the masonry infills. In this sense, the instrumentation comprised 13 independent nodes and 35 measured degrees of freedom or channels. In addition, the instrumentation setup was completed by two displacement transducers (LVDTs) placed at the keystone of the arch parallel to the movable edge and the infill in the opposite corner of the loading device. A geometrical scheme of the location of the accelerometers and LVDTs is illustrated in Figure 3.

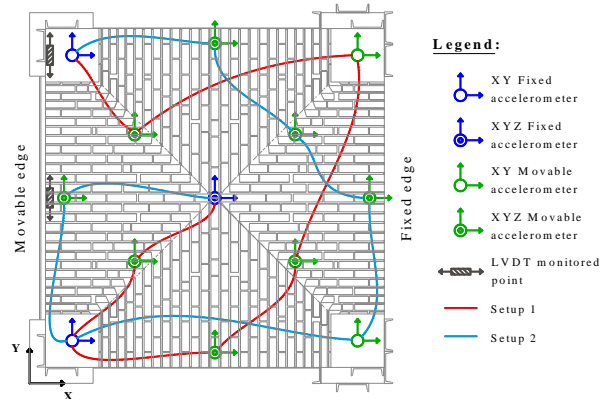


Figure 3. Location of the acceleration and displacement transducers.

3. METHODOLOGY

3.1. Quasi-static loading

The application of the cyclic loading was carried out considering a displacement-controlled approach. Following the guidelines provided by FEMA 461 [8], one movable edge of the CEB masonry cross-vault was subjected to horizontal and unidirectional displacements whose amplitude increased every two cycles. For assessing the cyclic response, 14 load sequences with displacements, whose values ranged between 0.5 mm and 39.7 mm, were considered. Before applying the first loading sequence, the base of the movable edge was covered with oil to reduce friction with the wheels. On the other hand, it is worth noting that the last loading sequence consisted of only one cycle since the specimen had already experienced severe damage and presented a high probability of collapse. The cyclic loading was applied at different rates, in which the velocities presented values starting from 1.0 mm/min to 30.0 mm/min for the first and last sequences. Table 1 summarises the displacement amplitudes and velocities for each loading sequence.

Table 1. History of displacement amplitude and velocity for the application of quasi-static cyclic loading.

| Sequence | 1 | 2 | 3 | 4 | 5 | 6 | 7 | 8 | 9 | 10 | 11 | 12 | 13 | 14 |
|-------------------|-----|-----|-----|-----|-----|-----|-----|-----|-----|------|------|------|------|------|
| Displacement (mm) | 0.5 | 0.7 | 1.0 | 1.4 | 1.9 | 2.7 | 3.8 | 5.3 | 7.4 | 10.3 | 14.5 | 20.2 | 28.4 | 39.7 |
| Velocity (mm/min) | 1.0 | 1.0 | 1.0 | 1.0 | 3.0 | 3.0 | 3.0 | 3.0 | 5.0 | 5.0 | 12.0 | 12.0 | 30.0 | 30.0 |

3.2. OMA-based damage detection

To assess the evolution of the dynamic properties, OMA tests were applied to the masonry cross-vault in different damage scenarios. The first corresponded to a reference scenario (RS) in which the vault did not experience any damage and was applied before the cyclic tests. Subsequently, seven damage scenarios (DS) were defined after two subsequent load sequences were applied. It is worth noting that each OMA test required the separation between the loading device and the movable support, aiming at neglecting its contribution to the dynamic properties of the specimen. For each OMA test, the ambient vibrations were acquired using the DEWESoftX [9] software, and it lasted 5 minutes with a sampling frequency of 500 Hz. The modal properties were identified using the EFDD method implemented in the software ARTeMIS Modal [10], considering a decimation upto to 50 Hz .

4. RESULTS

4.1. Cyclic response

From the hysteretic curves shown in Figure 4, it was possible to observe that the cyclic behaviour of the masonry cross-vault was characterised by a non-symmetrical response in terms of capacity and displacement registered by the LVDT at the keystone of the arch parallel to the movable edge. The maximum load capacity of the cross-vault was described by load factors (ratio between shear load and weight of the mock-up) of approximately 0.13 and 0.15 in +Y and -Y directions, respectively. These values were obtained at horizontal displacements around 7.45 mm and 10.13 mm in each case. In addition, the maximum horizontal displacement in the +Y corresponded to 27 mm, whereas in -Y, this value increased to 30 mm. This behaviour may be related to the application of the cyclic loads at one of the movable edges and the possible buckling of the steel bars in the +Y direction that did not allow a proper transmission of forces. On the other hand, it was evidenced that the post-peak response in both directions presented quite ductile behaviour with a slight reduction in the maximum load capacity. Based on the hysteretic curves, it was also possible to determine the material experienced stiffness and material degradation due to the loading and unloading cycles. Regarding cracking patterns, also shown in Figure 4, no significant damage was observed in the DS₁ and DS₂ scenarios since the cyclic response of the masonry cross-vault remained in the linear elastic field. A typical diagonal crack pattern started propagating from DS₃ at the centre of the specimen. In subsequent load sequences, additional cracks near the masonry infill became noticeable. The crack propagation continued until DS₇, in which a severe damage scenario was reached, preventing the completion of loading sequence 14.

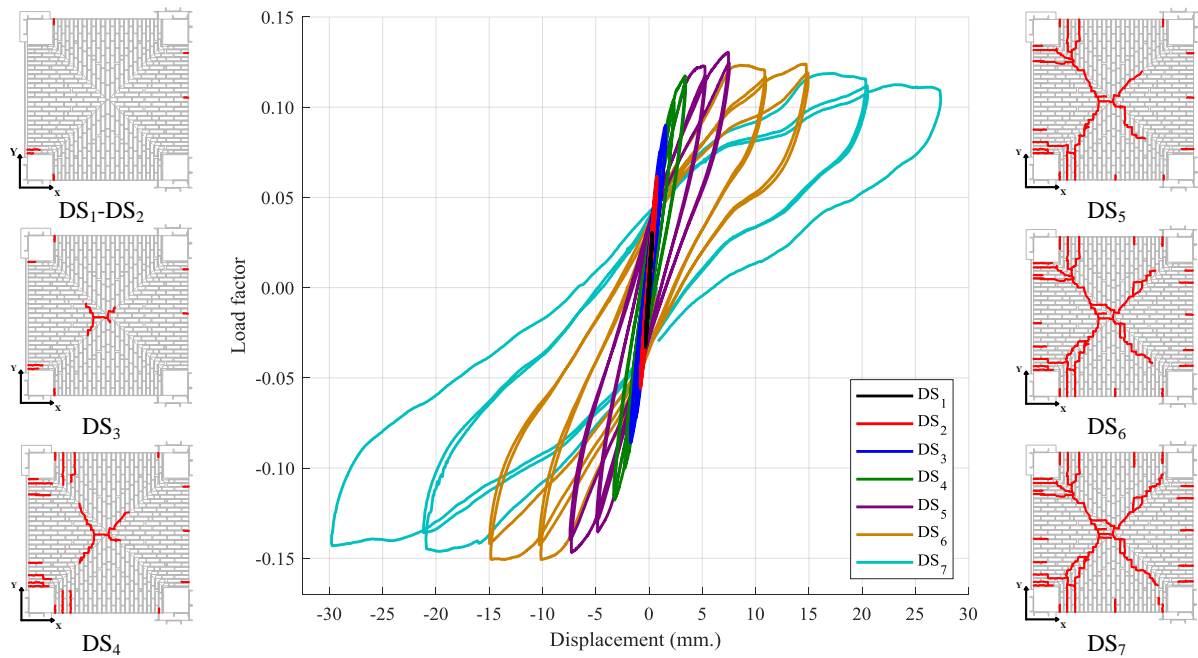


Figure 4. Hysteretic curves and crack patterns from the quasi-static cyclic loading test. Displacements were recorded at the keystone of the movable edge's arch.

4.2. Damage detection

The damage detection in the CEB masonry cross-vault required the identification of the dynamic properties in the undamaged conditions (RS) following a frequency domain approach. As illustrated in Figure 5a, the power spectral density was characterized by strong peaks between 10 Hz and 15 Hz which may be associated with well-defined vibration modes. It was also possible to observe another peak at 8 Hz with a lower amplitude which may indicate that such vibration was not properly excited by ambient vibrations. This behaviour was also observed in frequencies larger than 15 Hz. For this purpose, this researched focused only on the first three vibration modes (see Figure 5b).

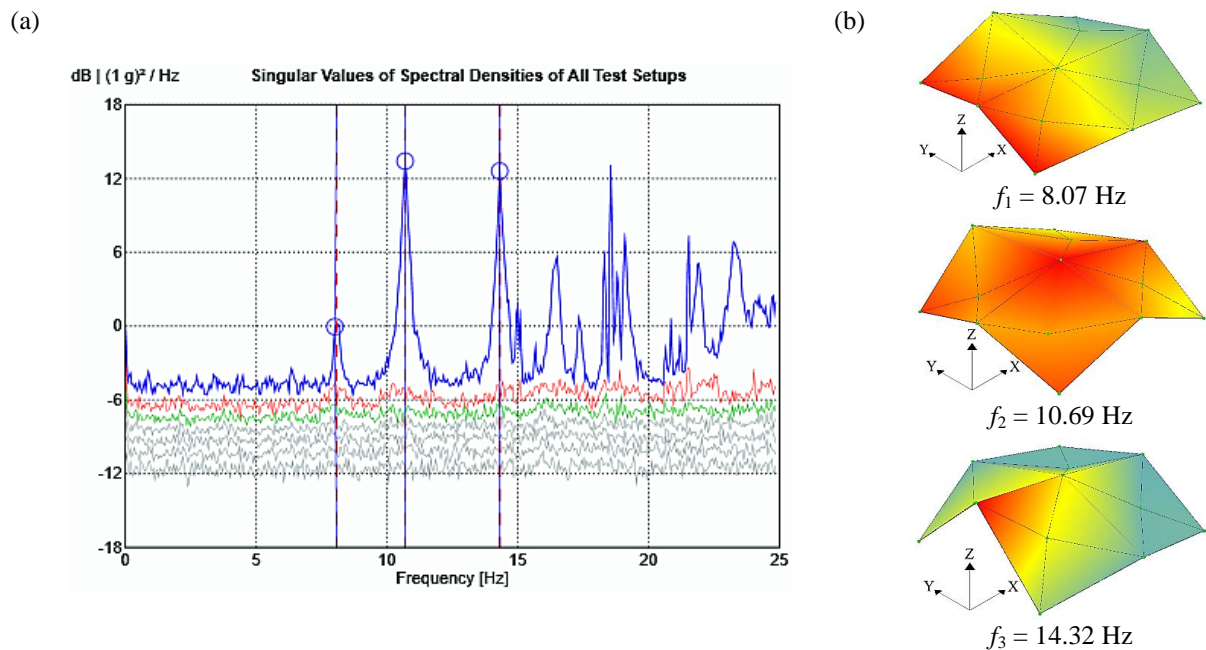


Figure 5. Modal identification of RS: (a) power spectral density. (b) first three vibration modes.

The first mode shape corresponded to a natural frequency of 8.07 Hz and was characterised by shear in-plane distortion, where the movable edge of the vault presented considerable lateral displacements in the Y-direction. On the other hand, the second one, corresponding to the frequency of 10.69 Hz, shows a pronounced vertical displacement of the vault central node and uniform horizontal displacements of the movable supports in the X-direction. Finally, the third vibration mode, with a frequency of 14.32 Hz, was described by the vertical displacement at the keystone of the arch of the movable edge that involved the horizontal displacements in opposite directions along the Y axis for the two movable supports. This behaviour may indicate the poor performance of the steel bars that connected the steel masses.

The damage in the cross-vault was assessed by estimating the changes in the dynamic properties of the first three vibration modes between the consecutive DSs. As reported in Table 2, it can be noted that the natural frequencies of all three vibration modes were characterised by a slight reduction between the RS and the DS₁ despite not experiencing any significant damage. This reduction ranged between 2% and 5%, and it can be attributed to a slight change in the boundary conditions at the base of the movable supports. It was noted that, for the application of the OMA tests in the undamaged conditions (before the first loading sequence), the wheels were not in direct contact with the oil, and therefore, the expected friction reduction did not take place at that stage. On the other hand, it was observed that the natural frequencies associated with DS₁ and DS₂ did not experience any significant changes, with percentual reductions of 3% and 5% in all modes. This reduction is strongly associated with the linear elastic behaviour of the CEB masonry cross-vault during the first load sequences. A higher reduction in frequency was observed throughout DS₃, DS₄ and DS₅, which varied between 8%-13%, 5%-9%, and 4%-8% for the first, second and third vibration modes, respectively. The natural frequencies of the first and second vibration modes presented a more pronounced reduction in the remaining DSs. For instance, the first vibration mode was characterised by a decrease of 19% and 24% for DS₆ and DS₇, respectively. In the case of the second vibration mode, the reduction in natural frequency was approximately 13% and 18% for each DS. Finally, the third vibration mode presented the slightest change of the three, presenting a frequency decrement of roughly 11%. These results showed that the most significant decrements in natural frequencies took place in the DS₆ and DS₇, in which the CEB masonry cross-vault presented severe cracking.

Table 2. Natural frequencies expressed in Hz. Percentual reduction with respect to RS in parentheses.

| Mode | DS ₁ | DS ₂ | DS ₃ | DS ₄ | DS ₅ | DS ₆ | DS ₇ |
|------|-----------------|-----------------|-----------------|-----------------|-----------------|-----------------|-----------------|
| 1 | 7.7 (5%) | 7.6 (5%) | 7.4 (8%) | 7.2 (10%) | 7.0 (13%) | 6.5 (19%) | 6.1 (24%) |
| 2 | 10.4 (3%) | 10.4 (3%) | 10.2 (5%) | 10.0 (6%) | 9.7 (9%) | 9.2 (13%) | 8.8 (18%) |
| 3 | 14.1 (2%) | 14.0 (3%) | 13.8 (4%) | 13.5 (6%) | 13.2 (8%) | 13.0 (10%) | 12.8 (11%) |

The damage detection on the vault was also assessed in terms of mode shape variations, calculating the MAC value between each DS and the RS (see Figure 6). It was possible to observe the MAC values exhibited a decreasing trend for all three vibration modes as the damage progressed. For instance, the second and third mode shapes presented similar behaviour, in which the MAC remained constant from DS₁ to DS₄. This behaviour was followed by a more pronounced MAC reduction in DS₅ to DS₇, in which the vault was characterised by severe damage. In this case, the minimum MAC values were 0.924 and 0.811 for the second and third vibration modes. On the other hand, the first vibration mode exhibited the lowest MAC values, with a maximum of 0.912 and a minimum of 0.749. It is worth noting that an unusual MAC increment was observed in DS₆, which may indicate that the mode shape presented a higher resemblance to the RS despite the degree of damage.

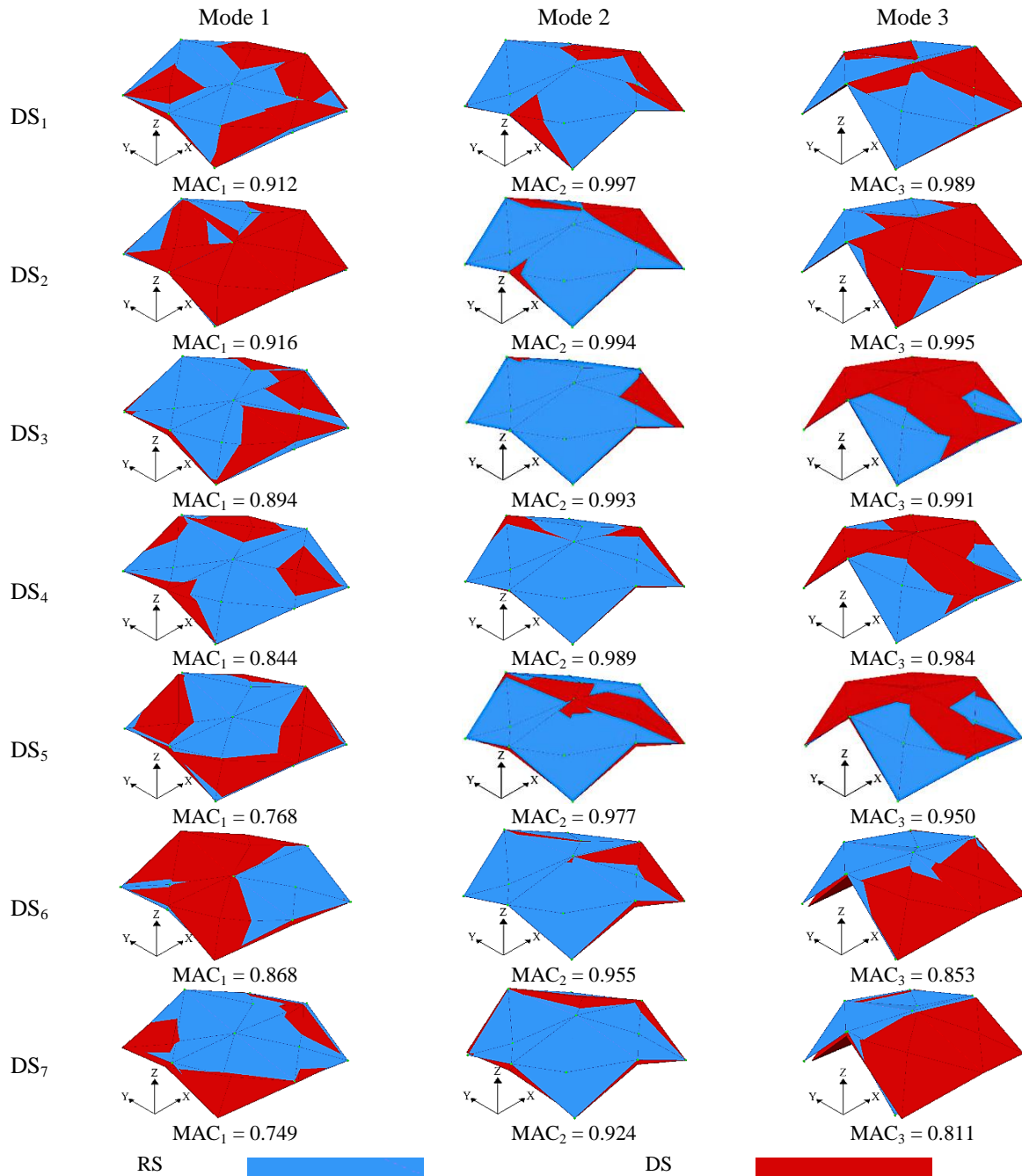


Figure 6. Modal shapes and MAC values comparison between each DS and RS

5. CONCLUSIONS

The paper presented the results of an experimental investigation of the structural behaviour of a full-scale CEB masonry cross-vault subjected to quasi-static cyclic loading tests. These analyses aimed at assessing the in-plane shear failure mechanism and its influence on the dynamic properties of the vault through different damage scenarios. The observed damage pattern strongly resembled the expected shear failure mechanism of masonry cross-vaults, namely diagonal cracking and the generation of plastic hinges. The hysteresis response demonstrated a gradual degradation of stiffness as damage accumulated, confirming the vulnerability of this structural typology under cyclic lateral loads. Operational Modal Analysis (OMA) was performed at different damage stages to evaluate changes in dynamic properties. A progressive reduction in natural frequencies was observed as damage increased, indicating stiffness degradation. Additionally, variations in mode shapes were assessed using the Mo-

dal Assurance Criterion (MAC), revealing significant changes in modal responses corresponding to crack development and propagation. The obtained results contribute to understanding the seismic vulnerability of CEB masonry cross-vaults and provide a basis for developing effective damage detection methodologies in historic and alternative masonry structures.

ACKNOWLEDGEMENTS

The authors would like to thank the financial support of the Peruvian CONCYTEC PROCIENCIA program with the fund PE501082211-2023. In addition, the authors would like to thank the support of the Earthquake-Resistant Structures Laboratory of the Engineering Department (LEDI) at the Pontificia Universidad Católica del Perú with the contract LE-CP-091-2024.

REFERENCES

- [1] Various authors, “Manuale per la compilazione della scheda per il rilievo del danno ai beni culturali, Chiese. MODELLO A-DC,” 2013. [Online]. Available: <https://www.protezionecivile.gov.it/it/pubblicazione/manuale-la-compilazione-della-scheda-il-rilievo-del-danno-ai-beni-culturali-chiese-modello-dc/>
- [2] N. Bianchini, N. Mendes, C. Calderini, P. Candeias, and P. B. Lourenço, “Shaking Table Testing of an Unstrengthened and Strengthened with Textile Reinforced Mortar (TRM) Full-Scale Masonry Cross Vault,” *International Journal of Architectural Heritage*, 2024, doi: 10.1080/15583058.2023.2295900.
- [3] E. Vintzileou, C. Mouzakis, L. Karapitta, and A. Miltiadou-Fezans, “Shake-Table Testing of a Cross Vault,” *Buildings*, vol. 12, no. 11, Nov. 2022, doi: 10.3390/buildings12111984.
- [4] D. Pellegrini, “Pre- and Post-Diction Simulation of the Seismic Response of a Masonry Cross Vault Tested on a Shaking Table,” *International Journal of Architectural Heritage*, pp. 1–21, Aug. 2023, doi: 10.1080/15583058.2023.2242812.
- [5] C. Chácará, B. Pantò, F. Cannizzaro, D. Rapicavoli, and I. Calì, “Numerical Simulation of the Response of an Unreinforced Brick-Masonry Cross Vault Subjected to Seismic Loading,” *International Journal of Architectural Heritage*, 2023, doi: 10.1080/15583058.2023.2290037.
- [6] R. Brincker, C. E. Ventura, and P. Andersen, “Damping Estimation by Frequency Domain Decomposition,” in *Proceedings of IMAC 19: A Conference on Structural Dynamics*, Hyatt Orlando, Kissimmee, Florida: Society for Experimental Mechanics, Feb. 2001, pp. 698–703. [Online]. Available: <https://vbn.aau.dk/en/publications/damping-estimation-by-frequency-domain-decomposition>
- [7] K. Huamani, R. Enciso, M. Gonzales, D. Zavaleta, and R. Aguilar, “Experimental and numerical evaluation of a stackable compressed earth block masonry system: Characterization at cyclic shear loads,” *Journal of Building Engineering*, vol. 60, Nov. 2022, doi: 10.1016/j.jobbe.2022.105139.
- [8] FEMA 461, “Interim Testing Protocols for Determining the Seismic Performance Characteristics of Structural and Nonstructural Components,” Washington D.C., Jun. 2007. [Online]. Available: www.ATCCouncil.org
- [9] DEWESoft®, “DEWESoftX,” 2024, Version 2024.4 (RELEASE-241001) (64-bit). [Online]. Available: <https://dewesoft.com/products/dewesoftx>
- [10] Structural Vibration Solutions, “ARTEMIS Modal 8.0,” Nov. 25, 2025, Aalborg, Denmark: Version 8.0.0.6-x64. [Online]. Available: <https://www.svibs.com/artemis-modal/>